doi:10.1111/evo.12185

MODULARITY AND RATES OF EVOLUTIONARY CHANGE IN A POWER-AMPLIFIED PREY CAPTURE SYSTEM

Thomas Claverie[1,2,3] and S. N. Patek[1,4]

[1]*Department of Biology, Organismic and Evolutionary Biology Graduate Program, University of Massachusetts, Amherst, Massachusetts*

[2]*Current address: Department of Evolution and Ecology, University of California, Davis, California*

[3]*E-mail: tclaverie@gmail.com*

[4]*Current address: Department of Biology, Duke University, Durham, North Carolina*

Received June 3, 2011
Accepted May 23, 2013
Data Archived: Dryad doi: 10.5061/dryad.67p

The dynamic interplay among structure, function, and phylogeny form a classic triad of influences on the patterns and processes of biological diversification. Although these dynamics are widely recognized as important, quantitative analyses of their interactions have infrequently been applied to biomechanical systems. Here we analyze these factors using a fundamental biomechanical mechanism: power amplification. Power-amplified systems use springs and latches to generate extremely fast and powerful movements. This study focuses specifically on the power amplification mechanism in the fast raptorial appendages of mantis shrimp (Crustacea: Stomatopoda). Using geometric morphometric and phylogenetic comparative analyses, we measured evolutionary modularity and rates of morphological evolution of the raptorial appendage's biomechanical components. We found that "smashers" (hammer-shaped raptorial appendages) exhibit lower modularity and 10-fold slower rates of morphological change when compared to non-smashers (spear-shaped or undifferentiated appendages). The morphological and biomechanical integration of this system at a macroevolutionary scale and the presence of variable rates of evolution reveal a balance between structural constraints, functional variation, and the "roles of development and genetics" in evolutionary diversification.

KEY WORDS: **Biomechanics, chronogram, integration, mantis shrimp, phylogenetic comparative methods, phylogenetic morphospace.**

The dynamic trio of evolutionary history, structural architecture, and function necessarily influence the patterns and processes of diversification (Thompson 1917; Raup 1966; Seilacher 1970; Lauder 1981; Gould 2002). One approach to analyzing the balance of these pressures is through the integration of phylogenetic analyses, biomechanics (the physical basis of movement and materials), and geometric morphometrics (analysis of the shape and size of functionally relevant structures). Here we integrate these areas by examining the association between evolutionary modularity (degree of evolutionary correlation) and rate of evolutionary change in a biomechanical system. Specifically, we measure and analyze the remarkably potent and evolutionarily diverse power amplification mechanism in mantis shrimp (Crustacea: Stomatopoda) raptorial appendages.

Modularity is defined as the relative correlation of components at genetic, developmental, functional, or evolutionary levels (Table 1; Klingenberg 2008b). Greater correlation indicates less modularity and lower correlation indicates greater modularity. A genetic module is a network of genes that leads to the expression of a particular trait (Mezey et al. 2000; Nadeau et al. 2003). Developmental modules are tissues that are coherent during their development due to genetic expression, cell communication, and

EVOLUTION
INTERNATIONAL JOURNAL OF ORGANIC EVOLUTION

Table 1. Four different types of modularity are defined in each row, then in each subsequent column the types of modularity are first placed conceptually in the context of an analysis of a power amplification mechanism, then presented with methods for detecting the particular type of modularity, and finally associated with examples in which these types of modularity have been detected (not necessarily in power amplification systems)

Modularity	Concept	Methods	Examples
Genetic modularity: Different genes or networks of genes are associated with engine, amplifier, and tool.	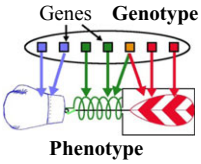	Engineered mutants, localized gene expression assays, quantitative trait loci analyses	**Crustacean mandibles** (Browne and Patel 2000) **Other** Rodent mandibles (Atchley and Hall 1991); Butterfly wing spots (Monteiro et al. 2003)
Developmental modularity: Engine, amplifier, and tool can have independent developmental pathways.	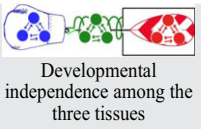	Morphological measurements, embryological measurements	**Raptorial appendages** (Claverie et al. 2011) **Other** Butterfly eyespots (Allen 2008); Rodent mandibles (Klingenberg et al. 2003)
Functional modularity: Engine, amplifier, and tool have different functions but are mechanically connected.	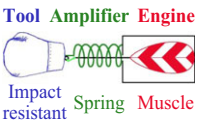	Biomechanical analyses	**Raptorial appendages** (Patek et al. 2007; Claverie et al. 2011) **Other** Chameleon tongues (de Groot and van Leeuwen 2004); Plant suction traps (Vincent et al. 2011)
Evolutionary modularity: Engine, amplifier, and tool evolve independently.	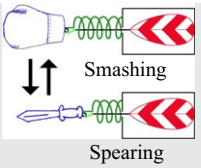	Phylogenetic comparison of morphological variation	**Raptorial appendages** Present work **Other** Rodent mandibles (Monteiro et al. 2005); Mammal skulls (Goswami 2006)

external stimuli (chemical or physical; Hallgrímsson et al. 2007). Functional modules are anatomical units of an organism that are used for a particular function (Moss 1968; Moss and Salentijn 1969; Zelditch et al. 2009). Finally, evolutionary modules correspond to the units of an organism that evolve independently from each other (Callebaut and Rasskin-Gutman 2005; Monteiro et al. 2005; Goswami 2006, 2007; Goswami and Polly 2010).

Evolutionary modularity, the focus of this study, emerges from the combined influence of genetic, developmental, and functional modularity over macroevolutionary timescales (Callebaut and Rasskin-Gutman 2005; Klingenberg 2008b). Previous work on mammal skulls suggests that functional modules (e.g., mandibles, orbits, vaults, molars, etc.) are also evolutionarily modular (Monteiro et al. 2005; Goswami 2006; Marroig et al. 2009; Porto et al. 2009; Drake and Klingenberg 2010; Goswami and Polly 2010). However, modularity at one level does not necessarily correspond to modularity at another level (e.g., genetic and functional modules might not match in their anatomical location; Cheverud 1982; Atchley and Hall 1991; Klingenberg et al. 2001; Magwene 2001; Klingenberg et al. 2003; Hulsey et al. 2005; Marquez 2008; Zelditch et al. 2009). For example, in cricket wings, genetic and developmental processes have low modularity, yet different regions of the wings have distinct functional modules for generating sound (Klingenberg et al. 2010).

The modularity of an organism has fundamental implications for the dynamics of evolution. Increased modularity may result in faster-evolving phenotypes that can be measured in terms of evolutionary rate. Evolutionary rate is the amount of morphological change within a taxon per unit of time; it is equivalent to phylogenetically standardized disparity (variance in shape) of the taxon (O'Meara et al. 2006). More broadly, modularity is hypothesized to enhance evolvability by reducing pleiotropic effects of the genome on the phenotype (Wagner 1996; Wagner and Altenberg 1996; Waxman and Peck 1998; Schlosser 2002; Snell-Rood et al. 2010).

We examine evolutionary modularity and rate of evolutionary change in a biomechanical mechanism called power amplification. Power amplification is a mechanism that reduces the time

needed to exert a force over a distance (work); the reduction in time is typically achieved through the use of springs and latches (Alexander and Bennet-Clark 1977; Alexander 1983; Gronenberg 1996; Patek et al. 2011). Power-amplified systems range from insect-catching chameleon tongues and the fast-closing mandibles of trap jaw ants to exploding fungal spores and the suction traps of carnivorous plants (de Groot and van Leeuwen 2004; Pringle et al. 2005; Patek et al. 2006, 2011; Vincent et al. 2011). Such systems are omnipresent, diverse, and have evolved multiple times in animals, plants, and fungi (e.g., Rothschild et al. 1972; Bennet-Clark 1975; Gronenberg 1996; Patek et al. 2004; Edwards et al. 2005; Lappin et al. 2006; Nüchter et al. 2006; Deban et al. 2007; Burrows et al. 2008; Van Wassenbergh et al. 2008; Noblin et al. 2009).

The building blocks of power-amplified systems naturally lend themselves to analyses of modularity. Three mechanical units (functional modules)—the engine, amplifier, and tool—characterize the mantis shrimp's power amplification system and virtually all other biological power-amplified systems (Claverie et al. 2011; Patek et al. 2011). The engine (e.g., muscle) performs work, the amplifier (e.g., spring and latch) stores elastic potential energy, and the tool serves as the device delivering the stored energy (e.g., foot or hammer). For example, mantis shrimp prepare for a raptorial strike by contracting forceful extensor muscles (engine) that compress the elastic region of the appendage's exoskeleton (amplifier) and store elastic potential energy (Fig. 1; Burrows 1969; Burrows and Hoyle 1972; Patek et al. 2004, 2007, 2013; Zack et al. 2009). To strike, the latches release and the stored elastic energy is transferred to the distal segments of the appendage that strike the prey (tool; Burrows 1969; Burrows and Hoyle 1972; Patek and Caldwell 2005; Patek et al. 2007; McHenry et al. 2012). Some mantis shrimp species can fracture hard-shelled prey with club-like appendages, earning them the name of "smashers"; others, called "spearers," stab fast-moving prey with spear-like appendages (Caldwell and Dingle 1976; Patek et al. 2004; Patek and Caldwell 2005; deVries et al. 2012). Mantis shrimp also wield variety of other "tools," including hatchets and other shapes that are intermediate between smashers and spearers (Ahyong 2001).

The physical rules of power amplification necessitate temporal and physical coordination among the engine, amplifier, and tool, whereas variation in the biomechanical performance of the system (i.e., differing speeds, accelerations, forces across species) may demand different amounts of coordination among these components. In other words, the engine, amplifier, and tool must be sufficiently integrated to successfully operate a mechanical system, yet the level of modularity might vary depending on the specialization or potency of the system (Table 1; Claverie et al. 2011; Patek et al. 2011). These principles may be relevant to the evolutionary diversification of power amplification in mantis shrimp. For example, smasher mantis shrimp exhibit far greater strike speeds, accelerations, and forces than non-smashers (Burrows and Hoyle 1972; Patek et al. 2004, 2007; Patek and Caldwell 2005; deVries et al. 2012). Smasher appendages also have greater muscle mass per unit size, more potent spring mechanisms, and a tool better suited to hammering than non-smashers (Authors unpublished data; Zack et al. 2009; Claverie et al. 2011; McHenry et al. 2012; Patek et al. 2013). In sum, all mantis shrimp

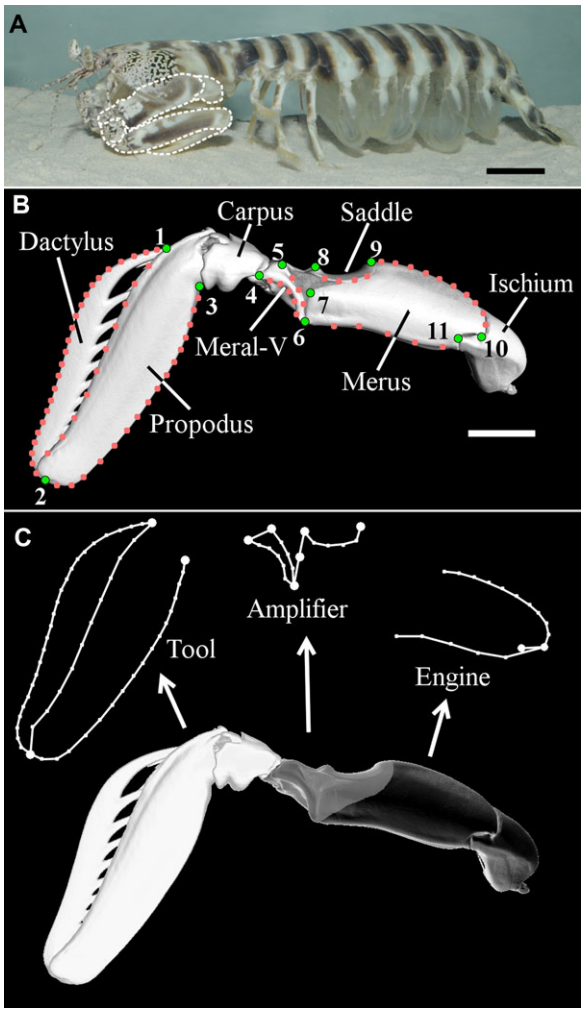

Figure 1. **The shape of the engine, amplifier and tool were measured across a wide range of mantis shrimp raptorial appendages. (A) A raptorial appendage is highlighted here in a spearing mantis shrimp (*Lysiosquillina glabriuscula*; white-dashed contour; anterior is to the left). (B) A computed tomography (CT) scan of a spearing raptorial appendage (*Lysiosquillina maculata*; closely related to *L. glabriuscula*; left appendage, distal to left) is overlaid with green points numbered from 1 to 11 which represent the landmarks digitized. The red points in between these landmarks represent the semi-landmarks. (C) These landmarks and semi-landmarks were partitioned to represent the engine, amplifier, and tool as indicated in the CT scan and line drawing. Scale bars are 2 cm. Computed tomography scan is adapted from deVries et al. (2012).**

require coordination among the engine, amplifier, and tool, but smashers may exhibit lower modularity than non-smashers to operate a substantially more powerful weapon.

Although the mechanical building blocks of power-amplified systems are well studied, far less is known about how such systems evolve and what processes underlie their remarkable macroevolutionary diversity. Claverie et al. (2011) found that the power amplification mechanism in mantis shrimp is modular at functional and developmental levels. They proposed, but did not test, the hypothesis that modularity of the engine, amplifier, and tool is correlated with rate of evolutionary change of these components and the overall biomechanical performance of the system. Thus, it is not yet known whether the engine, amplifier, and tool of power-amplified systems belong to one or separate evolutionary units and whether the level of evolutionary modularity influences rates of evolutionary change.

Toward the goal of integrating and quantitatively analyzing the roles of history, mechanics, and function in patterns of evolutionary diversification, we addressed two specific questions. First, are biomechanical components modular at the evolutionary level? Specifically, although previous research has shown that the biomechanical components of the mantis shrimp's power-amplified system (engine, amplifier, and tool) are developmentally modular within species (Claverie et al. 2011), we tested whether these same components are evolutionarily modular across mantis shrimp species and appendage types. Building on this first question, the second question asks whether greater modularity is associated with a higher rate of evolutionary change. We thus tested whether a higher level of modularity (lower evolutionary correlation among the engine, amplifier and tool) also occurs in groups with higher evolutionary rates of change of these components.

Materials and Methods

SAMPLES

A total of 281 specimens were measured from 58 species and 12 families (1–10 specimens per species, cf. Appendix). To maintain consistency with preservation artifacts, only museum specimens preserved in ethanol were used (National Museum of National History, Washington, DC, USA; Australian Museum of Natural History, Sydney, Australia; Rufino et al. 2004). Only adult specimens were measured to avoid any additional variation due to ontogenetic stages (Hartnoll 1982; Claverie and Smith 2009, 2010). Pictures of the left raptorial appendage's lateral side (Fig. 1) were taken in triplicate with an SLR camera (12 megapixel, digital SLR camera, Nikon D300; AF Micro-NIKKOR 60 mm f/2.8D or 105 mm f/2.8D macro lenses; Nikon Inc., Melville, NY; and EM-140 DG macro-flash, Sigma Corp., Ronkonkoma, NY). Two different macro lenses were used to accommodate the major size differences across species. The lenses were free from distortion and a scale bar was placed next to every appendage. Amplifiers (meral-V) were in a resting position in preserved animals, given that they require active muscle contraction with substantial force to rotate and compress before a strike (Fig. 1; Patek et al. 2007). Deformed appendages were not included. Total body length was measured with calipers (digital electronic vernier caliper, absolute coolant proof IP 67, $\pm$0.02 mm; Mitutoyo Corp., Kawasaki, Japan).

MORPHOLOGICAL MEASUREMENTS

Following a method nearly identical to Claverie et al. (2011), coordinates of points (landmarks and semi-landmarks) were digitized into two dimensions from the appendage photographs (Fig. 1). The only difference between the two studies is that semi-landmarks between landmarks 4 and 6 were added in this dataset. Appendage morphology was represented by a landmark configuration (the configuration made by all the digitized points for each picture). Following digitizing, landmark configurations were divided into three units representing the engine, amplifier, and tool (Fig. 1). Then, the differences in orientation, relative geometric position, and size among landmark configurations were removed using the generalized Procrustes superimposition procedure (Rohlf and Slice 1990). During superimposition, semi-landmarks were aligned (sliding) using the minimal bending energy method (Bookstein 1997).

We measured morphology in terms of both shape and size. Shape data were quantified using partial warp scores, which are multivariate values computed from the superimposed landmark configurations using the Thin Plate Spline interpolation function (Bookstein 1991). Size data were measured using centroid size, which is the scaling factor used to standardize landmark configurations during the superimposition procedure (Bookstein 1991). Both the partial warp scores and centroid sizes were computed with the software TPSRelw (Rohlf 2005).

PHYLOGENETIC DIVERGENCE TIME ESTIMATION

To analyze the correlation between traits across species via comparative methods, it is essential to know the phylogenic relationships among the species compared (Felsenstein 1985). Therefore, we used a stomatopod molecular phylogeny based on two nuclear (18S and 28S rDNA) and two mitochondrial (16S and cytochrome oxidase I) genes which was constructed using maximum likelihood heuristic searches (Porter et al. 2010).

Although the branch lengths in the Porter et al. (2010) phylogeny represent the number of nucleotide substitutions, in this study we used tests that assume branch lengths to be proportional to time. Therefore, the Porter et al. (2010) phylogeny was used to estimate a chronogram using the relaxed clock method and fossils were incorporated as hard boundaries (Table 2; Sanderson 2002). Branch lengths estimated by number of nucleotide substitutions,

Table 2. **Fossils and the associated dates that were used to calibrate seven nodes of the phylogeny. Also shown are the ages used in the analysis and the divergence times estimated by the analysis. Some fragments of modern stomatopod fossils were discovered from the middle Cretaceous, but could not be attributed with certainty to a particular family. Therefore, we could not assign an older age range for some families as indicated with "NA." The software r8s required one fixed node for cross validation; node 1 was fixed in the analysis to 300 Myr (age of the oldest fossil of the Stomatopoda ever discovered separating this group from Malacostraca) to meet this requirement. Fossils on nodes 3, 4, and 5 represent the oldest fossils found for Lysiosquilloidea, Pseudosquilloidea, and Squilloidea, respectively.**

Node	Species	Stratigraphy	Reference	Analysis age range (older–earlier)	Estimated age
1	*Tyrannophontes theridions*	Upper Pennsylvanian	(Schram 1969)	300–300 Myr	300 Myr
2	Various modern stomatopods	Middle Cretaceous	(Hof 1998)	100–55 Myr	86 Myr
3	*Lysiosquilla antigua*	Middle Eocene	(Secretan 1975)	NA-46 Myr	68 Myr
4	*Pseudosquilla wulfi*	Upper Eocene	(Förster 1982)	NA-33.7 Myr	59 Myr
5	*Squilla hollandi*	upper Eocene	(Förster 1982)	NA-33.7 Myr	51 Myr
6	*Gonodactylus oerstedii* (renamed *Neogonodactylus oerstedii*)	Miocene	(Rathbun 1935)	NA-10 Myr	24 Myr
7	"*Chloridella" empusa* (renamed *Squilla empusa*)	Pleistocene	(Rathbun 1935)	NA-0.2 Myr	11 Myr

as in the Porter et al. (2010) phylogeny, are a function of the mutation rate and the divergence time between two nodes. Therefore, to express branch lengths proportional to time, it is possible to calibrate ages of particular nodes by estimating mutation rate and using fossils (Sanderson 2002; Ho and Phillips 2009). Various models have been proposed to estimate mutation rates using either a molecular clock, a local clock, or a relaxed clock (Ho and Phillips 2009). We used the relaxed clock models, because they allow the occurrence of different mutation rates on different parts of the tree, with gradual transitions among these different rates (Sanderson 2002). When using relaxed clock models to estimate divergence times, it is also important to use fossils to date several well-distributed nodes across the phylogeny to minimize calibration error (Ho and Phillips 2009). To date such nodes, several methods such as point calibration, hard-bound and soft-bound calibration methods are available. We used hard-bound calibration over point calibration, because it allows some uncertainty in node age rather than setting a fixed age which is unrealistic considering the scattered nature of fossil records (Sanderson 2002; Wills 2007). Moreover, although soft-bound calibration is generally preferable to a hard-bound method, the soft-bound method requires estimation of the distribution in boundary uncertainty (e.g., logarithmic, normal, or exponential distribution), a task beyond the scope of this study (Yang and Rannala 2006; Ho and Phillips 2009).

The calibration of the Porter et al. (2010) phylogeny was done using the r8s program (Sanderson 2002). The smoothing parameter λ was set to 50 in agreement with a cross-validation procedure. The log penalty function was used instead of the additive function, because it leads to lower cross-validation scores which indicate better chronogram estimation (Sanderson 2002). Subsequently, a fossil cross-validation was performed to estimate whether there was incongruence in the calibration procedure (Near and Sanderson 2004). Seven nodes were calibrated using fossils (Fig. 2; Table 2). The root of the tree (node 1 on Fig. 2) corresponds to the separation between stomatopods and other crustaceans (outgroups from Porter et al. 2010). Given that most fossils are dated to an age range, the younger of each range was used as the earliest possible divergence time estimation.

Twenty-five species sampled in this study overlapped with the phylogeny of Porter et al. (2010); therefore, we pruned that phylogeny to only represent the focal species (Fig. 3, Mesquite version 2.72; Maddison and Maddison 2009).

EVOLUTIONARY MODULARITY

To determine if the engine, amplifier, and tool evolved independently, we tested whether morphological (shape and size) variation among these three regions was correlated across species. Phylogenetic comparative methods (independent contrasts) were used for this task, because morphological data were not independent across species (Felsenstein 1985). The shape data consisted of one averaged landmark configuration per species for the engine, amplifier, and tool. Size data consisted of the centroid size of the engine, amplifier, and tool, with one average value per species.

Independent contrasts assume that Brownian motion is a good evolutionary model for the variables measured and that there is phylogenetic signal in the data. Therefore, a Brownian motion model was tested by fitting various likelihood models of evolution to size and shape data (Procrustes distances to consensus) and the Akaike information criterion (AIC) was used to evaluate the best model. AIC ranks supported a Brownian motion model for these data.

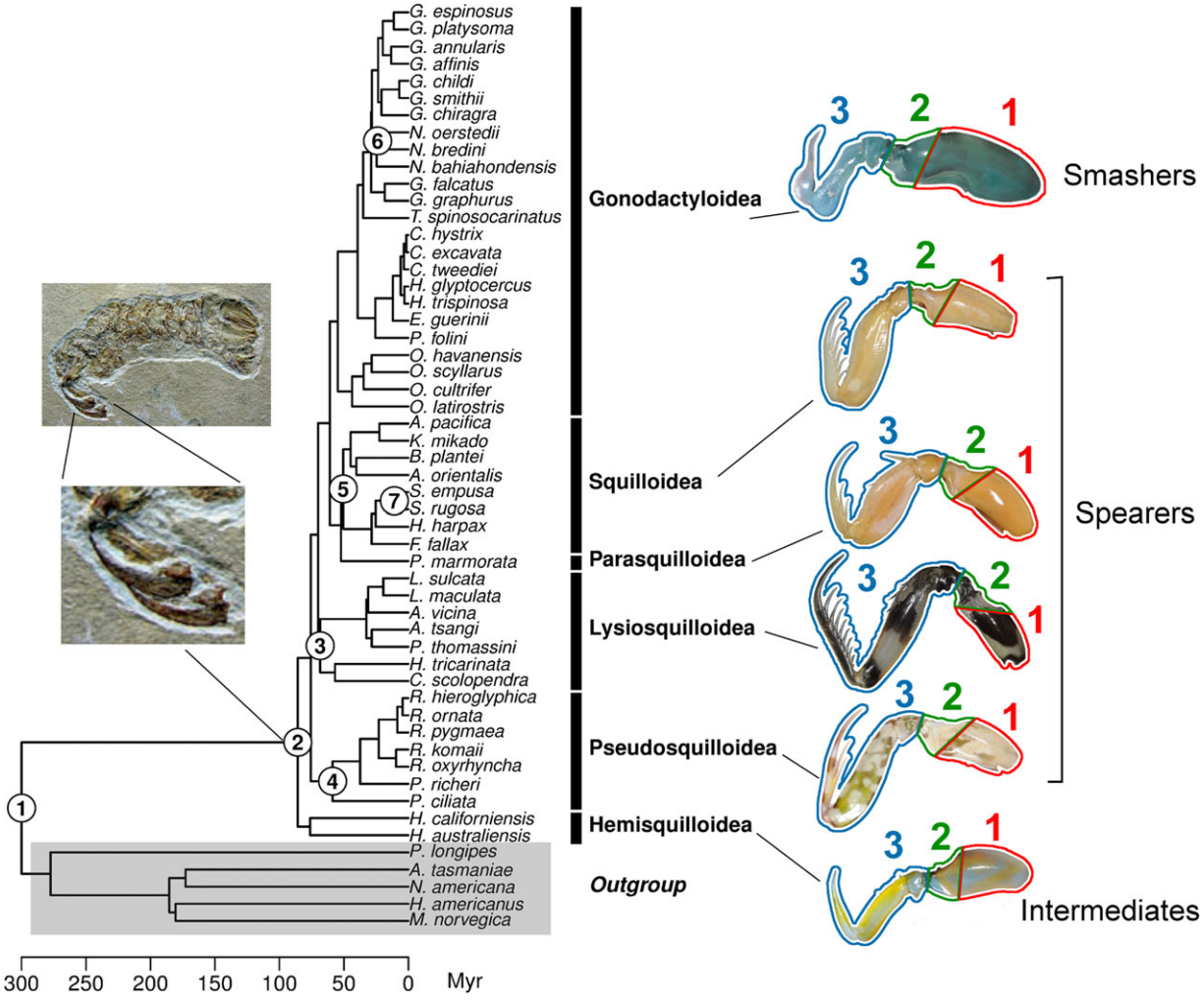

Figure 2. Mantis shrimp exhibit a range of appendage types, including smashers, spearers, and intermediates. To the right of the phylogeny, pictures of representative raptorial appendages and their functional classification (smashers, intermediates, and spearers) are displayed for each superfamily. Each appendage has the engine (red, 1), amplifier (green, 2), and tool (blue, 3) outlined. We incorporated fossil taxa as calibration points (node numbers represent each calibration point; Table 2) into this recently published phylogeny that includes the major superfamilies in the Stomatopoda (Porter et al. 2010). By incorporating fossils, we estimated the divergence times of mantis shrimp (scale: time before present in millions of years). *Archaeoscula phoenicia* is an ancestral species close to the root ancestor in this phylogeny; this fossil and its appendages are depicted in the photos to the left of the phylogeny (reprinted with permission, Ahyong and Jarman 2009; original photograph by A. Garassino). Outgroups used to root the phylogeny and stomatopod superfamilies are shown.

Phylogenetic signal was tested using separate methods for shape (multivariate data) and size (univariate data) of the engine, amplifier, and tool. For the size data, the centroid size of each module was first standardized by body length. Next, the phylogenetic signal was tested using Pagel's λ (Pagel 1999) as implemented in the package caper (previously CAIC) in R (Orme et al. 2012). For shape, the phylogenetic signal was tested using a permutation approach developed by Klingenberg and Gidaszewski (2010) because of the multivariate nature of the data. This was done with the software MorphoJ (Klingenberg 2008a). In light of the presence of phylogenetic signal (see Results), multivariate data (partial warps scores) and univariate data (standardized centroid size) were transformed using independent contrasts (Felsenstein 1985).

The second step tested whether shape and size were correlated across the engine, amplifier, and tool, again incorporating phylogeny. Different approaches were used for size and shape analyses. For size, the correlation among engine, amplifier, and tool was tested using major axis regression on the phylogenetic independent contrasts of size (Felsenstein 1985; Grafen 1989). For shape, two complementary methods were used to test for correlation: Mantel test and two block partial least squares analysis

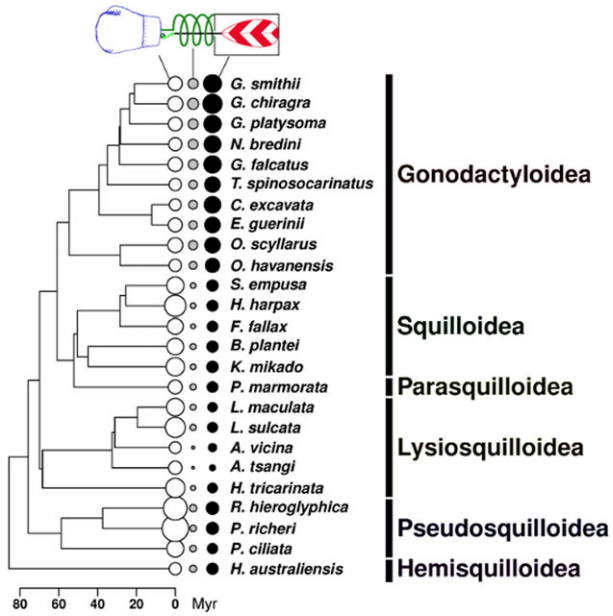

Figure 3. The correlated size evolution across power amplification components and across appendage types is evident in this phylogenetic mapping. Across all mantis shrimp, the engine sizes (black circles) and the amplifier sizes (gray circles) change concordantly, whereas the tool sizes (white circles) change independently (larger diameter circles indicate larger standardized size). Within smashers (Gonodactyloidea), all three components change similarly whereas the tool in the other taxa (non-smashers) is more variable relative to the engine and amplifier. We performed the phylogeny-based analyses using this pruned version of the chronogram depicted in Figure 2. Scale represents phylogenetic branch lengths in Myr (Porter et al. 2010).

(2B-PLS). In the first method, dissimilarity matrices for the engine, amplifier, and tool were calculated based on Euclidean distances among species and then the correlations among these dissimilarity matrices were tested using a Mantel test (VEGAN package; Oksanen et al. 2012). The results provided an estimate of the significance of the correlation of shape variation across the engine, amplifier, and tool incorporating phylogeny, but did not inform how the shape changes in the covariation (Monteiro et al. 2005; Zelditch et al. 2009; Claverie et al. 2011). Therefore, in the second method, a 2B-PLS was used to investigate how these sets of multivariate data covary (Rohlf and Corti 2000). The 2B-PLS analysis was used, because it extracts variables that account for the maximum covariation between two sets of multivariate data (Rohlf and Corti 2000). Such variables can subsequently be used to compute Thin Plate Spline deformation grids allowing a visualization of shape deformation associated with the covariation. Furthermore, 2B-PLS on independent contrasts of shape data indicates whether the shapes of the engine, amplifier, and tool covary across species independently from phylogenetic relationships. Finally, the Rv coefficient was used to evaluate the degree of correlation between each region's shape (Escoufier 1973). Simply put, the Rv coefficient is to the multivariate correlation as R^2 is to univariate data (Claude 2008; Escoufier 1973). The Rv coefficient has been used in other studies to show the degree of correlation between the shapes of two regions (Klingenberg 2009; Laffont et al. 2009). The Rv coefficient was computed using functions from Claude (2008) written in R (R Development Core Team 2009). The same dataset was used twice in different correlation analyses (multiple comparisons); therefore, a Bonferroni correction was applied when necessary (critical significance level was set to $P < 0.025$).

EVOLUTIONARY RATES

We measured the rate of morphological evolution of the engine, amplifier, and tool in smashers and non-smashers. The rate of morphological evolution is the time-independent variance parameter, σ^2, of the Brownian motion model of continuous character evolution; a greater Brownian rate means greater accumulation of disparity per unit of time (Felsenstein 1985; O'Meara et al. 2006). Shape was analyzed using the Procrustes distances between each species and the overall average shape configurations (Zelditch et al. 2004).

To enhance the power of the analysis beyond the 25 species used for the chronogram (see section "Phylogenetic Divergence Time Estimation"), we used the averaged shape of each of the 58 species. Calculation of rates requires having a fully resolved phylogeny including every species studied; however, in this analysis, we used more species than the ones available in the phylogeny (Appendix). Therefore, we included the additional species in the phylogeny as polytomies in their respective superfamilies. We then randomly resolved these polytomies using a birth–death model and generated 6000 trees following the Kuhn et al (2011) procedure in R and BEAST (R Development Core Team 2009, Drummond, 2012 #886).

Differences in rates of shape and size evolution were tested for the engine, amplifier, and tool between two groups: the smashers and the non-smashers. As will be presented in the Results, smashers (Gonodactyloidea) formed the least modular group and the non-smashers were more modular. "Brownie-lite" in the phytools package in R was used for this procedure. An AICc-based procedure was used to choose between a one rate model (same rate of evolution for each tested groups) or two rates model (different rates of evolution between the two groups tested). Finally, the rule of thumb that a ΔAICc > 4 offers substantial support for the best fitting model was employed (Burnham and Anderson 2002). The procedure was repeated 1000 times with each of the generated phylogenies and averages with confidence interval of estimated parameters were calculated.

PHYLOGENETIC MORPHOSPACE

Shape variation of the engine, amplifier, and tool across species was examined in a phylogenetic morphospace (Klingenberg and Gidaszewski 2010). We built the morphospace using a bivariate plot of the results of a PCA with the phylogenetic topology overlaid on the graph. Specifically, the PCA was run on a dataset consisting of 281 specimens from 58 species-level points, the 25 average species values from the tips of the chronogram and the reconstructed characters at the nodes of the chronogram. On the morphospace figure, the node and tip values were connected with line segments to illustrate the topology of the chronogram.

Results

EVOLUTIONARY MODULARITY

The shape and the standardized size of each region of the appendage exhibited phylogenetic signal (shape: 10,000 permutations, $P < 0.001$; size: $\lambda = 1$, $P < 0.001$). Therefore, independent contrasts were calculated for size and shape data (partial warp scores) before analysis.

Tests for correlations among engine, amplifier, and tool size yielded a weaker correlation between the tool and the other components and a stronger correlation between the engine and amplifier size. Thus, the tool formed one evolutionarily module and the engine and amplifier formed together another evolutionarily module. Specifically, the size of the engine was correlated with the size of the amplifier across species [reduced major axis regression slope is reported (intercept is set to 0 with independent contrasts) with a 95% interval and significance level based on 99 permutations: slope = 1.29(1.15–1.45), $P < 0.001$]; however, the size of the tool was neither correlated with engine size [slope = 0.33(0.25–0.44), $P = 0.282$] nor amplifier size [slope = 0.26(0.19–0.34), $P = 0.144$] (Figs. 3 and 4).

The correlations among the shapes of the engine, amplifier, and tool across species (independent contrasts) were analyzed using two different methods: distance matrix method and 2B-PLS method. Using the distance matrix method, it was found that the changes in shape across the engine, amplifier, and tool were all significantly correlated (Table 3). However, this result did not indicate which aspect of engine, amplifier, and tool shape drove this correlation. Therefore, a 2B-PLS analysis was performed to identify the shape covariation. The 2B-PLS results indicated that most of the covariation between the shape of the engine, amplifier, and tool was represented by the first axes (Fig. 5, Table 3). For these three comparisons, shape covariation was driven by the smashers (Gonodactyloidea), which have the most distinct engine, amplifier, and tool shapes when compared to the other superfamilies (cf. Figs. 5 and 6). Figure 6 shows that the shape of smasher appendages evolved toward a different area of the morphological space compared to other superfamilies. Further-

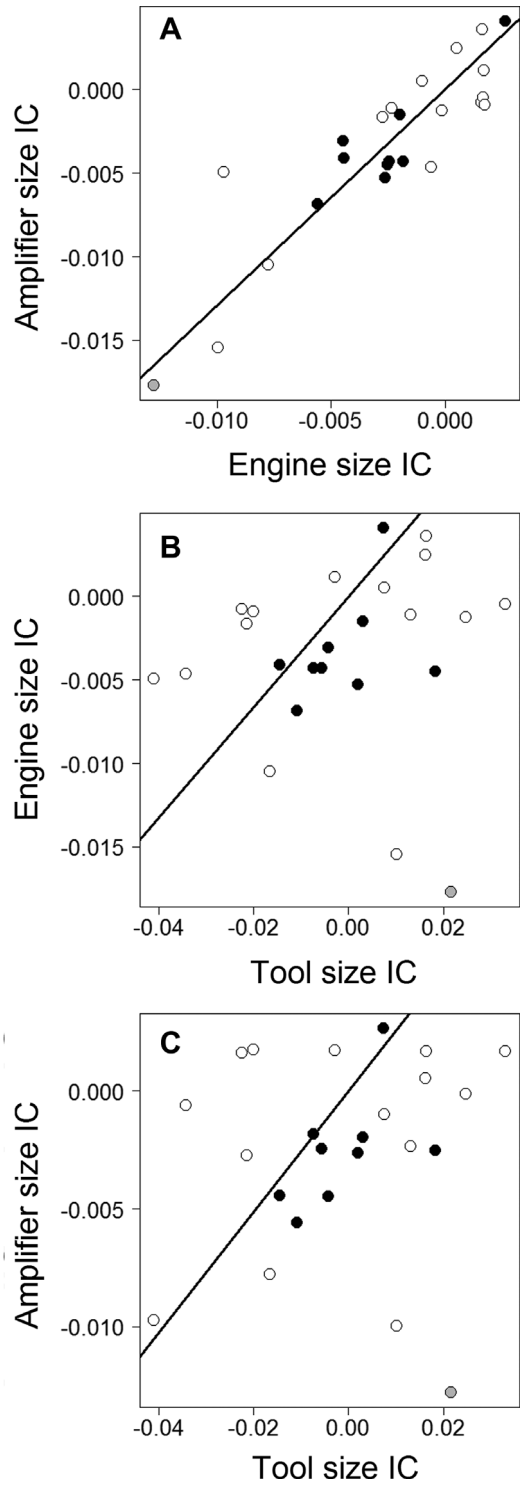

Figure 4. **The sizes of the power amplification regions are all positively correlated. Regressions of the independent contrast values (IC) are represented for the engine–amplifier size (A), the engine–tool size (B), and the amplifier–tool size (C). Reduced major axis regressions are used. The values are unit less, because they are contrasts from the centroid size (unit-less as well). Black dots represent smasher contrasts, white dots represent non-smasher contrasts, and the gray dot represents the ancestral contrast separating smashers from non-smashers.**

Table 3. Results of modularity analyses across the engine, amplifier, and tool. The first column indicates the shape comparisons and the subsequent three columns include the results. The second column indicates the results from the Mantel test and provides significance (computed with 1000 permutations) for the correlation of shape variation between regions across species (significance level is set at $P < 0.025$ due to a Bonferroni correction). Mantel statistics are based on Spearman's rank correlation ρ (r). The third column shows the percentage of covariation explained by each of the three first axes of the two block partial least squares analysis (2B-PLS) compared to the total covariation between the shapes of each region. The fourth column indicates the Rv coefficient that represents the strength of the correlation between the different regions. Rv = 0 means no correlation and Rv = 1 indicates a perfect correlation.

Comparisons	Mantel test results	2B-PLS axes – % of total covariation	Rv
Engine–Amplifier	$r = 0.54$ $P < 0.001$	1–67.46% 2–15.15% 3–5.41%	0.5187
Amplifier–Tool	$r = 0.31$ $P = 0.014$	1–52.11% 2–21.22% 3–9.30%	0.3947
Engine-Tool	$r = 0.38$ $P = 0.003$	1–60.09% 2–13.41% 3–9.99%	0.3407

more, even though shape variation between the engine, amplifier, and tool were significantly correlated, the Rv coefficient calculated between each region indicated a relatively weak correlation (maximum Rv = 0.52; Table 3). The same distance method analysis performed without smashers showed correlated shape variation between the engine and amplifier (Rv = 0.37, Mantel $r = 0.42$, $P < 0.001$), but no significant correlation between the engine and tool (Rv = 0.22, Mantel $r = 0.09$, $P = 0.250$) or the amplifier and tool (Rv = 0.40, Mantel $r = 0.17$, $P = 0.124$). Analyses with only smashers showed correlated variation between the engine–amplifier shape (Rv = 0.78, Mantel $r = 0.70$, $P < 0.001$), the engine–tool shape (Rv = 0.60, Mantel $r = 0.68$, $P < 0.001$), and the amplifier–tool shape (Rv = 0.46, Mantel $r = 0.64$, $P = 0.007$).

The same analyses were performed for size. Significant correlations were found for the non-smashers between engine–amplifier [slope = 1.04(0.84–1.30), $P < 0.001$], amplifier–tool [slope = 0.18(0.13–0.26), $P = 0.004$], and engine–tool [slope = 0.19(0.13–0.27), $P = 0.001$]. With only the smashers, engine–amplifier size was correlated [slope = 1.31(1.09–1.57), $P < 0.001$] whereas amplifier–tool size [slope = 0.36(0.22–0.56), $P = 0.030$] and engine–tool size were not significantly correlated [slope = 0.46(0.29–0.75), $P = 0.078$].

EVOLUTIONARY RATES

We compared evolutionary rates between groups with different levels of modularity. We found that smashers (Gonodactyloidea), which were less modular than non-smashers, exhibited a slower rate of change in both size and shape compared to non-smashers. AICc model selection showed that a two rate model is preferable to a one rate model for the shape of engine (ΔAICc = 4.49), amplifier (ΔAICc = 5.73), and tool (ΔAICc = 11.65). The engine, amplifier, and tool shape evolved at a rate that was at least 10 times higher for the non-smashers (Fig. 7; engine rate: $1.13 \times 10^{-3} \pm 2.32 \times 10^{-2}$ SD, amplifier rate: $2.85 \times 10^{-4} \pm 2.02 \times 10^{-3}$ SD, tool rate: $1.19 \times 10^{-3} \pm 1.97 \times 10^{-2}$ SD) compared to the smashers (Fig. 7; engine rate: $1.31 \times 10^{-4} \pm 3.03 \times 10^{-4}$ SD, amplifier rate: $3.86 \times 10^{-5} \pm 2.32 \times 10^{-5}$ SD, tool rate: $9.71 \times 10^{-5} \pm 4.18 \times 10^{-4}$ SD). A similar pattern was found for the rate of size evolution, although only tool rate was significantly different between the two groups (engine, ΔAICc = 3.50; amplifier, ΔAICc = 2.21; tool, ΔAICc = 5.27). Rates of size evolution were always larger for non-smashers (Fig. 7; engine rate: $1.99 \times 10^{-4} \pm 2.67 \times 10^{-3}$ SD, amplifier rate: $1.84 \times 10^{-4} \pm 2.75 \times 10^{-3}$ SD, tool rate: $1.03 \times 10^{-3} \pm 1.18 \times 10^{-2}$ SD) than for smashers (Fig. 7; engine rate: $1.22 \times 10^{-4} \pm 2.61 \times 10^{-4}$ SD, amplifier rate: $2.97 \times 10^{-5} \pm 2.48 \times 10^{-3}$ SD, tool rate: $1.85 \times 10^{-4} \pm 5.78 \times 10^{-4}$ SD).

Discussion

Our goal of integrating biomechanics, function, and macroevolution while addressing broad questions about modularity and rates of evolutionary change, yielded several key findings about the mantis shrimp's power amplification system. Our first question addressed the variation in the modularity of the engine, amplifier, and tool. We found that evolutionary shape variation is correlated across the engine, amplifier, and tool components. Thus, the components of this power amplification system exhibit relatively low evolutionary modularity. When we compared smashers to non-smashers, the smashers were less evolutionarily modular than non-smashers. Our second question addressed whether greater modularity is associated with higher rates of evolutionary change. We found that the less evolutionarily modular smashers evolved more slowly than non-smashers, which supports previous predictions that greater modularity is correlated with greater rate of evolutionary change. These results also support the notion that the more biomechanically potent performance of smashers was accompanied by a decrease in modularity of the components, perhaps because of increased temporal and mechanical coupling among the mechanical components. In the course of this Discussion, we will examine these results and interpret them in the broader context of understanding the dynamics of evolutionary diversification.

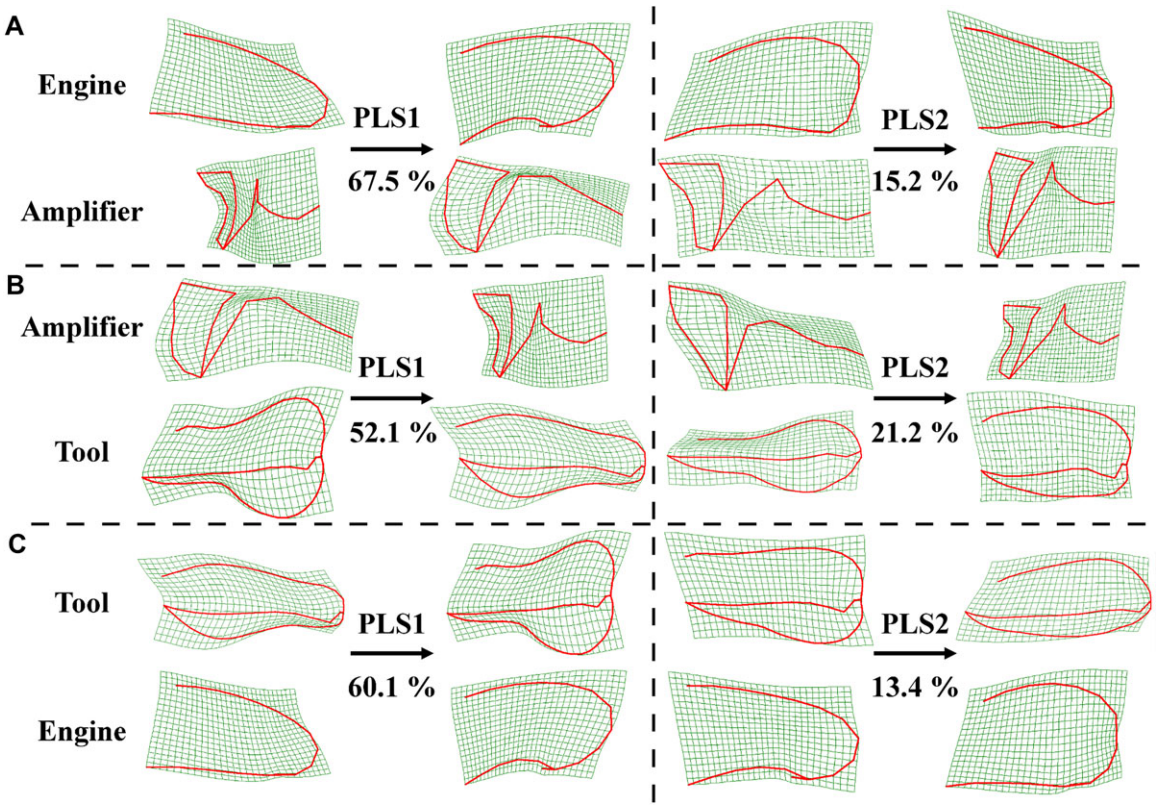

Figure 5. When considering covariation of shape evolution, one can compare the two major axes of covariation (left column: first partial least square; right column: second partial least square) in terms of (A) engine vs. amplifier, (B) amplifier vs. tool, and (C) tool vs. engine. These deformations are placed in the context of superfamily relationships and appendage types in the phylogenetic morphospace depicted in Figure 6. Numbers indicate the percentage of covariation explained by the different axes. Shape differences are expressed as deformations of the average shape by using thin-plate splines. Landmarks are connected with line segments to facilitate visualization (cf. Fig. 1).

MODULARITY

Our current and previous analyses of modularity span developmental and evolutionary levels, taxonomic groupings (smashers and non-smashers), and functional modules/biomechanical units (engine, amplifier and tool). Although these multiple approaches and levels of analysis can make interpretation of the results complicated, we will step through these findings and explain how these multilevel analyses can yield insight into the evolutionary processes and patterns underlying biomechanical and morphological diversity.

We begin by considering the broadest level of analysis which combined all taxa and appendage types. In these analyses, the results for shape differed from the results for size. The strongest statistical support was found for the shape analyses, which showed that evolutionary variation among the engine, amplifier, and tool was correlated. These results thus demonstrate coevolution of the three regions and, thus, relatively low evolutionary modularity. The analysis of size showed that tool variation was not correlated with the amplifier and engine variation. Because the smashers' appendage shape was so distinct from the non-smashers (Fig. 6), the smashers disproportionately influenced these findings and we thus split the dataset into smashers and non-smashers for further analysis.

With the smashers separated from the non-smashers, a different set of patterns emerged. When only considering the non-smashers, evolutionary variation in tool shape was not correlated with engine and amplifier shape; however, evolutionary changes in size of the engine, amplifier, and tool were correlated. When just the smashers were included, evolutionary changes in the shape of the engine, amplifier, and tool were correlated, but tool size did not change with engine and amplifier size.

Across these analyses, two possible patterns emerge: the engine, amplifier, and tool coevolved (i.e., one evolutionary module) or the tool evolved independently from the engine and amplifier (i.e., two evolutionary modules). Although these results rule out many other hypothesized scenarios (e.g., engine, amplifier and tool form three evolutionary modules), the question remains: did the tool coevolve with the engine and amplifier or did it evolve

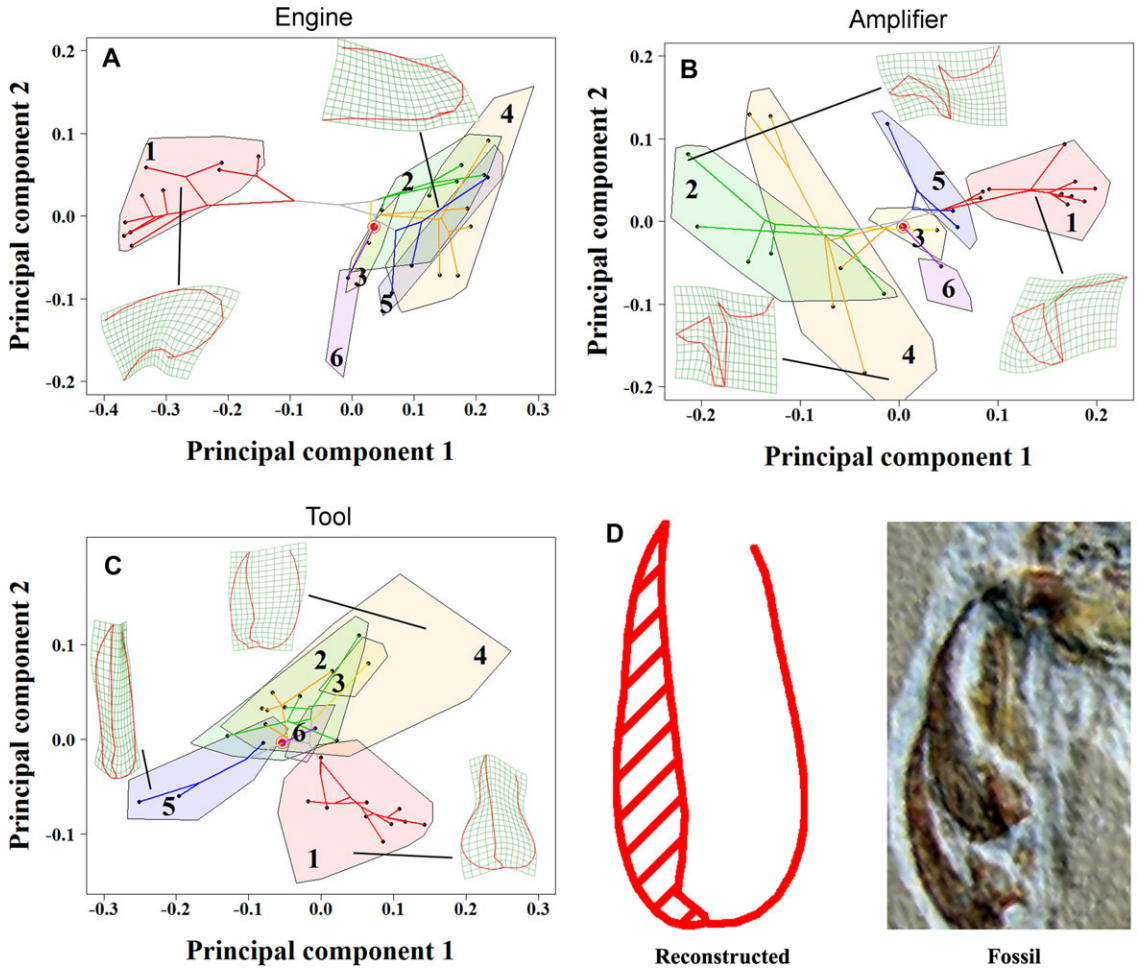

Figure 6. The shape of the engine (A), amplifier (B), and tool (C) are distinct in smashers (1, red) compared to non-smashers when viewed in these phylogenetic morphospaces. The deformation grids represent shape variation at the extremes of the morphospace. Variance explained by the first and second principal components are respectively 83.10% and 9.13% for the engine, 56.58% and 24.63% for the amplifier, 44.60% and 26.71% for the tool. The larger circled dot (red) in each graph represents the root shape reconstruction. The node positions in the cladogram correspond to the reconstructed shape of common ancestors. The polygons represent the distribution of every specimen measured per superfamily, encompassing all of the data used in the evolutionary rates analyses. The averaged species data (black dots) were used for the modularity analyses. The identity of the superfamilies are as follows: 1 (red), Gonodactyloidea; 2 (green), Squilloidea; 3 (yellow), Parasquilloidea; 4 (orange), Lysiosquilloidea; 5 (blue), Pseudosquilloidea; 6 (purple), Hemisquilloidea. The reconstructed tool shape of the root ancestor using the squared-change parsimony criterion is shown in D side by side with the picture of the fossil shown in Figure 3 (authorized reproduction of the photograph taken by A. Garassino as depicted in Ahyong and Jarman 2009). Two tools on top of each other were fossilized and only the dactyl (hatched region in the reconstructed configuration) is visible.

independently? The statistical results were strongest for the shape analyses. For the shape dataset including all taxa as well as the dataset only including smashers, the engine, amplifier, and tool coevolved and thus form one evolutionary module. The shape dataset only including the non-smashers supported independent evolution of the tool, and, thus, two evolutionary modules. Thus, the shape data suggest different patterns of evolutionary modularity in smashers compared to non-smashers and the Stomatopoda as a whole. The size results were less statistically robust; the independent contrast regression slopes were relatively low and the scatterplots were diffuse (Fig. 4). Given the greater statistical support for shape compared to the size results, we base our subsequent interpretation of the results on the evolution of shape.

Mantis shrimp exemplify the fact that types of modularity can be distinct from each other (see Introduction and Table 1). We defined the engine, amplifier, and tools as three functional modules. Our evolutionary modularity analysis pinpointed either one or two evolutionary modules, and analysis of modularity within a smasher species (*Gonodactylaceus falcatus*) revealed the engine, amplifier, and tool as three developmental modules

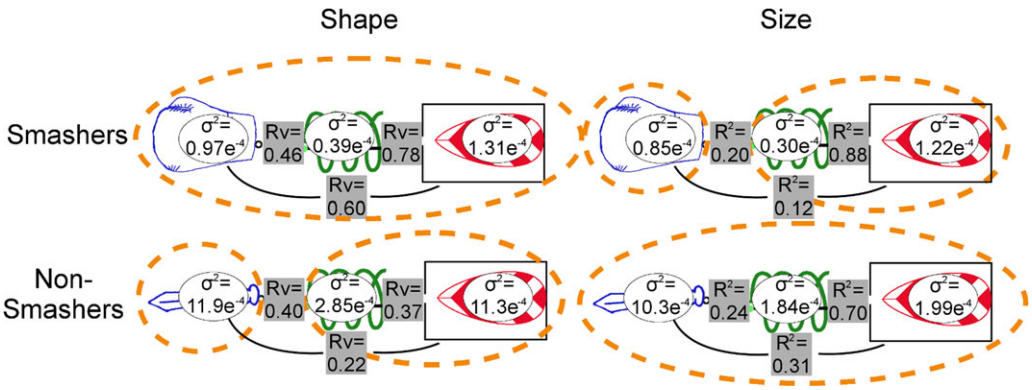

Figure 7. **When comparing shape evolution between smashers and non-smashers (left column), lower levels of modularity are associated with lower rates of evolutionary change (orange dashed ellipses group coevolving components). Specifically, the level of shape modularity is low is smashers (gray boxes: high Rv correlation level) and rates of evolutionary change are low (white circles: low σ^2 evolutionary rate). In non-smashers, the level of shape modularity between the tool and other components is relatively high (low Rv) and the rates of evolutionary change are 10-fold higher for all components compared to the smashers. When comparing size evolution (right column), the results shown here are statistically significant, but are less strongly supported. The lower R^2 values are likely due to greater size data scatter, particularly between in the tool vs. engine and tool vs. amplifier comparisons (see Fig. 4B, C). Similar to the shape comparisons, the rate of size evolution is greater in the non-smashers compared to the smashers.**

(Claverie et al. 2011). In sum, depending on the type of modularity, the mantis shrimp's power amplification system consists of either one, two, or three modules. How can these results be reconciled?

If the rules of arthropod limb development drive modularity, then each segment should be a developmental module, because different genes are expressed on a proximo-distal axis in early development (Browne and Patel 2000; Prpic and Damen 2009). For example, the development of the distal portion of a crustacean appendage is dictated by *Distalless* (dll) gene expression (Browne and Patel 2000). Similarly, in grasshoppers, *Extradenticle* (Exd) gene expression controls the development of the proximal domain of their appendages whereas *Distalless* controls the distal portion (Jockusch et al. 2000; Williams and Nagy 2001). The finding of developmental modularity among the engine, amplifier, and tool supports this role of developmental processes. Alternatively, the engine and amplifier belong to the same segment (merus) and may thus be less modular relative to each other than with the tool, which consists of separate segments (propodus and dactylus; cf. Fig. 1); this pattern of modularity was reflected in our evolutionary modularity results. Clearly, further research is needed to parse the role of developmental mechanisms in these patterns of modularity, in addition to examination of the other potential influences, such as environmental constraints or the development of adjacent tissues (Smith and Palmer 1994; Nijhout and Emlen 1998).

Alternatively, one might consider the evolutionary pressures on this system and their role in the modularity of the engine, amplifier, and tool. From a biomechanical or structural perspective, greater performance of a system may require more robust connections among the biomechanical components, such that shifting evolutionary pressures across the clade may yield different patterns of evolutionary modularity. One obvious consideration in mantis shrimp is the different strike performance between the highly potent smashers and the slower, less forceful non-smashers. Smashers break hard shelled prey with strikes exceeding 20 m s^{-1} and forces reaching 1500 N. Spearers strike soft, evasive prey that do not require crushing force and their strikes are both slower (on the order of 5 m s^{-1}) and weaker (Patek et al. 2004; Patek and Caldwell 2005; deVries et al. 2012). Some spearer superfamilies have species with large adults (over 40-cm long) that generate strikes with a large reach (>10 cm), particularly in the Squilloidea and Lysiosquilloidea. Their weaker springs and greater leverage supplied by their large appendages might be sufficient to generate satisfactory speed to capture prey without power amplification (deVries et al. 2012; Patek et al. 2013). Although untested biomechanically at this point, it is possible that the greater spring and strike performance necessitated greater temporal and spatial linkages among the components in smashers, ultimately leading to lower modularity across the engine, amplifier, and tool in smashers compared to non-smashers.

These different pressures at the developmental and evolutionary levels may have shifted over the history of the clade. Given the ubiquity of developmental control patterns in arthropods, it is likely that developmental modularity was present and dominant in the early phases of the evolution of raptorial appendages. Subsequent specialization for extremely high speeds and impact forces may have shifted the dynamics to a greater influence of mechanical and physical constraints, thereby promoting less modularity among the components. Although speculative at this point, one possible scenario is that developmental modularity set the stage

for the evolutionary origin and subsequent diversification of the power amplification mechanism by allowing traits to evolve independently. When the power amplification system shifted toward more potent mechanical coupling, both modularity and diversification rate decreased.

One final consideration is the theory of "correlated progression" (Kemp 2007). Kemp (2007) proposed that, in some systems, functional demands on a particular trait must reach a threshold before associated traits change. Similarly, in power-amplified systems, it is possible that selective pressures on the tool had to reach a threshold before causing correlated evolutionary change in the engine and amplifier. The associated changes in the engine and amplifier were necessary to maintain mechanical integration and thus, whereas the engine, amplifier, and tool emerged as a single evolutionary module, the tool was slightly decoupled from this evolutionary pattern.

EVOLUTIONARY RATES

Although the causal connections between modularity and evolutionary rates are not established, theoretical predictions suggest that higher modularity in organisms should lead to greater evolvability which would be manifested as a higher rate of evolution (Wagner 1996; Wagner and Altenberg 1996). Indeed, mantis shrimp with greater evolutionary modularity exhibit a higher rate of evolution. Even with substantial morphological variability (Fig. 7), a 10-fold higher evolutionary rate was found independently in each of the engine, amplifier, and tool of the non-smashers (more modular) when compared to smashers (less modular). Similarly, lower modularity was correlated with lower disparity in studies of mammal skulls (this study used disparity as a proxy for evolvability; Goswami and Polly 2010). Although morphological disparity is influenced by phylogenetic structure, and is therefore not an ideal proxy for evolutionary rate (O'Meara et al. 2006), these results are consistent with our findings and corroborate the argument that greater modularity is linked to greater rate of evolution.

Our findings, which to our knowledge are the first to address evolutionary modularity in nonmammalian structures, provide an interesting point of comparison with the developmental, functional, and evolutionary modularity seen in mammal skulls. Mammalian developmental modules are mostly consistent across taxa; for example, most mammals show distinct developmental modularity between the cranium and the facial bones (Goswami 2006; Hallgrímsson et al. 2007; Drake and Klingenberg 2010). Furthermore, higher disparity in various skull regions appears to be associated with greater modularity (Goswami and Polly 2010), possibly due to differential selective pressures (Monteiro et al. 2005; Drake and Klingenberg 2010; Goswami and Polly 2010). For example, the functional and mechanical decoupling of the facial bones and the cranium likely allows these two modules to evolve independently (Moss 1968; Moss and Salentijn 1969; Callebaut and Rasskin-Gutman 2005; Monteiro et al. 2005; Goswami 2006; Goswami 2007; Goswami and Polly 2010). In another related example, the greater skull disparity and variation in the facial bones of domestic compared to wild canids (Drake and Klingenberg 2010) may have resulted from reduced selection on function and mechanics due to domestication and artificial selection, thereby permitting greater variation.

The engine, amplifier, and tool of power-amplified systems may also experience varying intensity of selective pressures due to shifting functions of the whole system and its component parts. For example, spearers in the Lysiosquilloidea and Squilloidea either do not use their amplifiers or the amplifiers are less effective (deVries et al. 2012; Patek et al. 2013). The release from or reduction of selection on the function or mechanical couplings of the engine, amplifier and tool, may have permitted greater evolutionary modularity and greater rates of evolutionary change in these groups. In another intriguing example, the semilunar process (Bennet-Clark 1975) is used as an amplifier in locusts, but not in grasshoppers or false stick insects (Burrows and Wolf 2002; Burrows and Morris 2003). False stick insects and grasshoppers have such long legs that their muscles generate sufficient takeoff velocity without the need for power amplification (Burrows and Wolf 2002; Burrows and Morris 2003). Similarly, hopping mice and kangaroos have power-amplified hind legs; however, hopping mice do not use their amplifier because muscle elasticity is sufficient relative to animal mass to store the elastic energy necessary for jumping (Biewener et al. 1981; Ettema 1996). Future studies of modularity in these systems may reveal similar associations between modularity, disparity, selection, and evolutionary rates.

PHYLOGENETICS AND PHYLOGENETIC MORPHOSPACE

Although each superfamily exhibits a homogenous assortment of raptorial appendage shapes consistent with recent phylogenies (Ahyong and Jarman 2009; Porter et al. 2010), our results show that smashers (Gonodactyloidea; Fig. 3) followed an evolutionary path that led to unique, hammer-shaped raptorial appendages. The smashers occupy a distinct region of the morphospace for the engine, amplifier, and tool (Fig. 6) compared to other superfamilies [including the non-smashers Hemisquilloidea and Pseudosquilloidea, formerly classified within Gonodactyloidea (Ahyong 2001)], and thus our results also support the reclassification of Gonodactyloidea (defined in Porter et al. 2010). Smashers are morphologically distinct, not just in terms of their hammer-shaped appendages, but also because of their enlarged engine and unique amplifier configuration (a medial saddle, straight meral-V, and small gap proximal to the meral-V). These findings echo biomechanical and physiological studies that have shown that

smashers have greater muscle force (M. Blanco and S. N. Patek, in review) and more robust springs than found in non-smashers (Patek et al. 2013).

The shape reconstruction presented in this study is necessarily influenced by our choice of parameters and assumptions. Our methods assume Brownian motion and a "true" phylogeny, whereas the distinct region of the morphospace colonized by the Gonodactyloidea suggests a directional model of evolution, such as an Ornstein–Uhlenbeck model (Butler and King 2004). However, our tests consistently supported a Brownian Motion model and other stomatopod phylogenies confirm Porter et al.'s (2010) tree topology (Ahyong and Harling 2000; Ahyong and Jarman 2009). Fossilized raptorial appendages look similar to extant taxa and the common ancestor to all extant species possessed raptorial appendages (Hof 1998; Haug et al. 2010). Therefore, our results may have differed slightly, but not substantially, if we had used other reconstruction methods. In future studies, Bayesian analyses could enhance the probabilistic assessment of these models and reconstructions.

Conclusions

Modularity and rates of evolutionary change of the engine, amplifier, and tool are likely driven by changes in the underlying network of genetic pathways, the mechanical limits imposed by the temporal and spatial coupling of these components, and shifts in selective pressures on behavioral function. The finding that the relatively lower modularity of the engine, amplifier, and tool is associated with a lower rate of evolution supports classic predictions of modularity and evolvability while also invoking classic arguments about the role of physical and mechanical constraints on the functioning of biological systems. This study thus offers new perspectives on arthropod evolution, the diversification of biomechanical systems, and the timeless roles of structural architecture, phylogenetic history, and function underlying the dynamics of organismal evolution.

ACKNOWLEDGMENTS

The authors are especially grateful to D. Cloutier, Q. Tran, and J. Yonamine for their help with digitizing. K. Reed and the staff of the Department of Invertebrate Zoology, National Museum of Natural History, Washington, DC, and S. Keable, Marine Invertebrate Collection, Australian Museum of Natural History in Sydney were very helpful during museum visits. For training in phylogenetic comparative methods, the authors thank the AnthroTree Workshop (supported by National Science Foundation BCS-0923791) and C. Nunn. The authors thank S. Price for her extremely helpful advice on phylogenetic comparative methods. We greatly appreciate M. Porter's help and guidance with dating the phylogeny. M. Zelditch gave helpful advice in geometric morphometric methods and J. Claude offered both advice and R code related to geometric morphometric methods. The Behaviour and Morphology group at the University of Massachusetts, Amherst, provided constructive comments on the manuscript. The authors greatly appreciate the constructive comments of four anonymous reviewers. This research was funded by a National Science Foundation Integrative Organismal Systems grant (#1014573 to SNP). The authors declare that they have no competing financial interests.

LITERATURE CITED

Ahyong, S. T. 2001. Revision of the Australian stomatopod crustacea. Australian Museum, Sydney.

Ahyong, S. T., and C. Harling. 2000. The phylogeny of the stomatopod crustacea. Aust. J. Zool. 48:607–642.

Ahyong, S. T., and S. N. Jarman. 2009. Stomatopod interrelationships: preliminary results based on analysis of three molecular loci. Arthropod Syst. Phylogeny 67:91–98.

Alexander, R. M. 1983. Animal mechanics. Blackwell Scientific Publications, Boston.

Alexander, R. M., and H. C. Bennet-Clark. 1977. Storage of elastic strain energy in muscle and other tissues. Nature 265:114–117.

Allen, C. E. 2008. The "Eyespot Module" and eyespots as modules: development, evolution, and integration of a complex phenotype. J. Exp. Z. Part b: Mol. Develop. Evol. 310B:179–190.

Atchley, W. R., and B. K. Hall. 1991. A model for development and evolution of complex morphological structures. Biol. Rev. Cambridge Philos. Soc. 66:101–157.

Bennet-Clark, H. C. 1975. The energetics of the jump of the locust *Schistocerca gregaria*. J. Exp. Biol. 63:53–83.

Biewener, A. A., R. M. Alexander, and H. C. Heglund. 1981. Elastic energy storage in the hopping of kangaroo rats (*Dipodomys spectabilis*). J. Zool. 195:369–383.

Bookstein, F. L. 1991. Morphometric tools for landmark data, geometry and biology. Cambridge Univ. Press, Cambridge, U.K.

———. 1997. Landmark methods for forms without landmarks: morphometrics of group differences in outline shape. Med. Image Anal. 1:225–243.

Browne, W. E., and N. H. Patel. 2000. Molecular genetics of crustacean feeding appendage development and diversification. Semin. Cell Develop. Biol. 11:427–435.

Burnham, K. P., and D. R. Anderson. 2002. Model selection and multimodel inference: a practical information theoretic approach. Springer, New York.

Burrows, M. 1969. The mechanics and neural control of the prey capture strike in the mantid shrimps *Squilla* and *Hemisquilla*. Zeitschrift für Vergleichende Physiologie 62:361–381.

Burrows, M., and G. Hoyle. 1972. Neuromuscular physiology of the strike mechanism of the mantis shrimps, *Hemisquilla*. J. Exp. Zool. 179:379–394.

Burrows, M., and O. Morris. 2003. Jumping and kicking in bush crickets. J. Exp. Biol. 206:1035–1049.

Burrows, M., and H. W. Wolf. 2002. Jumping and kicking in the false stick insect *Prosarthia teretrirostris*: kinematics and motor control. J. Exp. Biol. 205:1519–1530.

Burrows, M., S. R. Shaw, and G. P. Sutton. 2008. Resilin and chitinous cuticle form a composite structure for energy storage in jumping by froghopper insects. BMC Biol. 6:41.

Butler, M. J., and A. A. King. 2004. Phylogenetic comparative analysis: a modeling approach for adaptive evolution. Am. Nat. 164:683–695.

Caldwell, R. L., and H. Dingle. 1976. Stomatopods. Sci. Am. 234:81–89.

Callebaut, W., and D. Rasskin-Gutman. 2005. Modularity: understanding the development and evolution of natural complex systems. Pp. 455. The Vienna series in theoretical biology. The MIT Press, Cambridge.

Cheverud, J. M. 1982. Phenotypic, genetic, and environmental morphological integration in the cranium. Evolution 36:499–516.

Claude, J. 2008. Morphometrics with R. Springer, New York.

Claverie, T., and I. P. Smith. 2009. Morphological maturity and allometric growth in the squat lobster *Munida rugosa*. J. Marine Biol. Assoc UK 89:1189–1194.

———. 2010. Allometry and sexual dimorphism in the chela shape in the squat lobster *Munida rugosa*. Aquat. Biol. 8:179–187.

Claverie, T., E. Chan, and S. N. Patek. 2011. Modularity and scaling in fast movements: power amplification in mantis shrimp. Evolution 65:443–461.

de Groot, J. H., and J. L. van Leeuwen. 2004. Evidence for an elastic projection mechanism in the chameleon tongue. Proc. R. Soc. Lond. Ser. B-Biol. Sci. 271:761–770.

Deban, S. M., J. C. O'Reilly, U. Dicke, and J. L. Van Leeuwen. 2007. Extremely high-power tongue projection in plethodontid salamanders. J. Exp. Biol. 210:655–667.

deVries, M., E. A. K. Murphy, and S. N. Patek. 2012. Strike mechanics of an ambush predator: the spearing mantis shrimp. J. Exp. Biol. 215:4374–4384.

Drake, A. G., and C. P. Klingenberg. 2010. Large-scale diversification of skull shape in domestic dogs: disparity and modularity. Am. Nat. 175:289–301.

Edwards, J., D. Whitaker, S. Klionsky, and M. J. Laskowski. 2005. A record-breaking pollen catapult. Nature 435:164.

Escoufier, Y. 1973. Le traitement des variables vectorielles. Biometrics 29:751–760.

Ettema, G. J. C. 1996. Elastic and length-force characteristics of the gastrocnemius of the hopping mouse (*Notomys Alexis*) and the rat (*Rattus norvegicus*). J. Exp. Biol. 199:1277–1285.

Felsenstein, J. 1985. Phylogenies and the comparative method. Am. Nat. 125:1–15.

Förster, M. V. R. 1982. Stomatopods (Crustacea, Hoplocarida) from the Eocene of northern Germany and the Maastrichtian of Nigeria. Neues Jahrbuch für Geologie und Paläomtologie, Monatshefte 6: 321–335.

Goswami, A. 2006. Cranial modularity shifts during mammalian evolution. Am. Nat. 168:270–280.

———. 2007. Cranial modularity and sequence heterochrony in mammals. Evol. Develop. 9:290–298.

Goswami, A., and P. D. Polly. 2010. The influence of modularity on cranial morphological disparity in Carnivora and primates (Mammalia). PLoS One 5:e9517–e9517.

Gould, S. J. 2002. The structure of evolutionary theory. Harvard Univ. Press, Cambridge, MA.

Grafen, A. 1989. The phylogenetic regression. Philos. Trans. R. Soc. Lond. Ser. B-Biol. Sci. 326:119–157.

Gronenberg, W. 1996. Fast actions in small animals: springs and click mechanisms. J. Comparat. Physiol. A-Neuroethol. Sens. Neural Behav. Physiol. 178:727–734.

Hallgrímsson, B., D. E. Lieberman, W. Liu, A. F. Ford-Hutchinson, and F. R. Jirik. 2007. Epigenetic interactions and the structure of phenotypic variation in the cranium. Evol. Develop. 9:76–91.

Hartnoll, R. G. 1982. Growth. Pp. 111–196 *in* D. E. Bliss, ed. The biology of Crustacea. Vol. 2. Embryology, morphology, and genetics. Academic Press, New York.

Haug, J. T., C. Haug, A. Mass, V. Kutschera, and D. Waloszek. 2010. Evolution of mantis shrimps (Stomatopoda, Malacostraca) in the light of new Mesozoic fossils. BMC Evol. Biol. 10:290.

Ho, S. Y. W., and M. J. Phillips. 2009. Accounting for calibration uncertainty in phylogenetic estimation of evolutionary divergence times. Syst. Biol. 58:367–380.

Hof, C. H. J. 1998. Fossil stomatopods (Crustacea: Malacostraca) and their phylogenetic impact. J. Nat. Hist. 32:1567–1576.

Hulsey, C. D., G. J. Fraser, and J. T. Streelman. 2005. Evolution and development of complex biomechanical systems: 300 million years of fish jaws. Zebrafish 2:243–257.

Jockusch, E. L., C. Nulsen, S. J. Newfeld, and L. M. Nagy. 2000. Leg development in flies versus grasshoppers: differences in *dpp* expression do not lead to differences in the expression of downstream components of the leg patterning pathway. Development 127:1617–1626.

Kemp, T. S. 2007. The concept of correlated progression as the basis of a model for the evolutionary origin of major new taxa. Proc. R. Soc. Lond. Ser. B-Biol. Sci. 274:1667–1673.

Klingenberg, C. P. 2008a. MorphoJ. Faculty of life science. Manchester University, Manchester, U.K.

———. 2008b. Morphological integration and developmental modularity. Ann. Rev. Ecol., Evol. Syst. 39:115–132.

———. 2009. Morphometric integration and modularity in configurations of landmarks: tools for evaluating *a priori* hypotheses. Evol. Develop. 11:405–421.

Klingenberg, C. P., A. V. Badyaev, S. M. Sowry, and N. J. Beckwith. 2001. Inferring developmental modularity from morphological integration: analysis of individual variation and asymmetry in bumblebee wings. Am. Nat. 157:11–23.

Klingenberg, C. P., and N. A. Gidaszewski. 2010. Testing and quantifying phylogenetic signals and homoplasy in morphometric data. Syst. Biol. 59:245–261.

Klingenberg, C. P., M. Katharina, and J. C. Auffray. 2003. Developmental integration in a complex morphological structure: how distinct are the modules in the mouse mandible? Evol. Develop. 5:522–531.

Klingenberg, C. P., V. Debat, and D. A. Roff. 2010. Quantitative genetics of shape in cricket wings: developmental integration in a functional structure. Evolution 64:2935–2951.

Kuhn, T. S., A. O. Mooers, and G. H. Thomas. 2011. A simple polytomy resolver for dated phylogenies. Methods Ecol. Evol. 2:427–436.

Laffont, R., E. Renvoisé, N. Navarro, P. Alibert, and S. Montuire. 2009. Morphological modularity and assessment of developmental processes within the vole dental row (*Microtus arvalis*, Arvicolinae, Rodentia). Evol. Develop. 11:302–311.

Lappin, A. K., J. A. Monroy, J. Q. Pilarski, E. D. Zepnewski, D. J. Pierotti, and K. C. Nishikawa. 2006. Storage and recovery of elastic potential energy powers ballistic prey capture in toads. J. Exp. Biol. 209:2535–2553.

Lauder, G. V. 1981. Form and function: structural analysis in evolutionary morphology. Paleobiology 7:430–442.

Maddison, W. P., and D. R. Maddison. 2009. Mesquite: a modular system for evolutionary analysis. Version 2.73. Available at http://mesquiteproject.org.

Magwene, P. M. 2001. New tools for studying integration and modularity. Evolution 55:1734–1745.

Marquez, E. 2008. A statistical framework for testing modularity in multidimensional data. Evolution 62:2688–2708.

Marroig, G., L. T. Shirai, A. Porto, F. B. de Oliveira, and V. De Conto. 2009. The evolution of modularity in the mammalian skull II: evolutionary consequences. Evol. Biol. 36:136–148.

McHenry, M. J., T. Claverie, M. V. Rosario, and S. N. Patek. 2012. Gearing for speed slows the predatory strike of a mantis shrimp. J. Exp. Biol. 215:1231–1245.

Mezey, J. G., J. M. Cheverud, and G. P. Wagner. 2000. Is the genotype-phenotype map modular? A statistical approach using mouse quantitative trait loci data. Genetics 156:305–311.

Monteiro, A., J. Prijs, M. Bax, T. Hakkaart, and P. M. Brakefield. 2003. Mutants highlight the modular control of butterfly eyespot patterns. Evol. Develop. 5:180–187.

Monteiro, L. R., V. Bonato, and S. F. dos Reis. 2005. Evolutionary integration and morphological diversification in complex morphological structures: mandible shape divergence in spiny rats (Rodentia, Echimyidae). Evol. Develop. 7:429–439.

Moss, M. L. 1968. Functional cranial analysis of mammalian mandibular ramal morphology. Acta Anatom. 71:423–447.

Moss, M. L., and L. Salentijn. 1969. Primary role of functional matrices in facial growth. Am. J. Orthodont. 55:566–577.

Nadeau, J. H., L. C. Burrage, J. Restivo, Y. H. Pao, G. Churchill, and B. D. Hoit. 2003. Pleiotropy, homeostasis, and functional networks based on assays of cardiovascular traits in genetically randomized populations. Genome Res. 13:2082–2091.

Near, T. J., and M. J. Sanderson. 2004. Assessing the quality of molecular divergence time estimates by fossil calibrations and fossil-based model selection. Philos. Trans. R. Soc. Lond. Ser. B-Biol. Sci. 359:1477–1483.

Nijhout, H. F., and D. J. Emlen. 1998. Competition among body parts in the development and evolution of insect morphology. Proc. Natl. Acad. Sci. USA 95:3685–3689.

Noblin, X., S. Yang, and J. Dumais. 2009. Surface tension propulsion of fungal spores. J. Exp. Biol. 212:2835–2843.

Nüchter, T., M. Benoit, U. Engel, S. Özbek, and T. W. Holstein. 2006. Nanosecond-scale kinetics of nematocyst discharge. Curr. Biol. 16:R316–R318.

O'Meara, B., C. Ané, M. J. Sanderson, and P. C. Wainwright. 2006. Testing for different rates of continuous trait evolution using likelihood. Evolution 60:922–933.

Oksanen, J., F. G. Blanchet, R. Kindt, P. Legendre, P. R. Minchin, R. B. O'Hara, G. L. Simpson, P. Solymos, M. Henry, H. Stevens, and H. Wagner. 2012. vegan: Community Ecology. Package. R package version 2.0-4. Available at http://CRAN.R-project.org/package=vegan.

Orme, D., R. Freckleton, G. Thomas, T. Petzoldt, S. Fritz, N. Isaac and W. Pearse. 2012. caper: Comparative Analyses of Phylogenetics and Evolution in R. R package version 0.5. Available at http://CRAN.R-project.org/package=caper.

Pagel, M. 1999. Inferring the historical patterns of biological evolution. Nature 401:877–884.

Patek, S. N., and R. L. Caldwell. 2005. Extreme impact and cavitation forces of a biological hammer: strike forces of the peacock mantis shrimp *Odontodactylus scyllarus*. J. Exp. Biol. 208:3655–3664.

Patek, S. N., W. L. Korff, and R. L. Caldwell. 2004. Deadly strike mechanism of a mantis shrimp. Nature 428:819–820.

Patek, S. N., J. E. Baio, B. L. Fisher, and A. V. Suarez. 2006. Multifunctionality and mechanical origins: ballistic jaw propulsion in trap-jaw ants. Proc. Natl. Acad. Sci. USA 103:12787–12792.

Patek, S. N., B. N. Nowroozi, J. E. Baio, R. L. Caldwell, and A. P. Summers. 2007. Linkage mechanics and power amplification of the mantis shrimp's strike. J. Exp. Biol. 210:3677–3688.

Patek, S. N., D. M. Dudek, and M. V. Rosario. 2011. From bouncy legs to poisoned arrows: elastic movements in invertebrates. J. Exp. Biol. 214:1973–1980.

Patek, S. N., M. V. Rosario, and J. R. A. Taylor. 2013. Comparative spring mechanics in mantis shrimp. J. Exp. Biol. 215:1317–1329.

Porter, M. L., Y. Zhang, S. Desai, R. L. Caldwell, and T. W. Cronin. 2010. Evolution of anatomical and physiological specialization in the compound eyes of stomatopod crustaceans. J. Exp. Biol. 213:3473–3486.

Porto, A., F. B. de Oliveira, L. T. Shirai, V. De Conto, and G. Marroig. 2009. The evolution of modularity in the mammalian skull I: morphological integration patterns and magnitudes. Evol. Biol. 34:118–135.

Pringle, A., S. N. Patek, M. Fischer, J. Stolze, and N. P. Money. 2005. The captured launch of a ballistospore. Mycologia 97:866–871.

Prpic, N. M., and W. G. M. Damen. 2009. *Notch*-mediated segmentation of the appendages is a molecular phylotypic trait of the arthropods. Develop. Biol. 326:262–271.

R Development Core Team. 2009. R: A language and environment for statistical computing. R Foundation for Statistical Computing, Vienna, Austria.

Rathbun, M. J. 1935. Fossil Crustacea of the Atlantic and Gulf coastal plain. Geol. Soc. Am. (Special Paper) 2:160.

Raup, D. M. 1966. Geometric analysis of shell coiling: general problems. J. Paleontol. 40:1178–1190.

Rohlf, F. J. 2005. Tpsrelw, relative warps. Department of Ecology and Evolution, State University of New York at Stony Brook, Stony Brook, NY.

Rohlf, F. J., and M. Corti. 2000. Use of two-block partial least-squares to study covariation in shape. Syst. Biol. 49:740–753.

Rohlf, F. J., and D. Slice. 1990. Extensions of the Procrustes method for the optimal superimposition of landmarks. Syst. Zool. 39:40–59.

Rothschild, M., Y. Schlein, K. Parker, and S. Sternberg. 1972. Jump of the oriental rat flea *Xenopsylla cheopis* (Roths.). Nature 239: 45–48.

Rufino, M. M., P. Abello, and A. B. Yule. 2004. The effect of alcohol and freezing preservation on carapace size and shape in Liocarcinus depurator (Crustacea, Brachyura). Pp. 45–53 *in* A. M. T. Elewa, ed. Morphometrics-applications in biology and paleontology. Springer-Verlag, Berlin.

Sanderson, M. J. 2002. Estimating absolute rates of molecular evolution and divergence times: a penalized likelihood approach. Mol. Biol. Evol. 19:101–109.

Schlosser, G. 2002. Modularity and the units of evolution. Theory Biosci. 121:1–80.

Schram, F. R. 1969. Polyphyly in the Eumalacostraca? Crustaceana 16:243–250.

Secretan, S. 1975. Les crustacés du Monte Bolca. Studi e ricerche sui giacimenti terziari di Bolca 2:315–388.

Seilacher, A. 1970. Arbeitskonzept zur Konstruktions-Morphologie. Lethaia 3:393–396.

Smith, L. D., and A. R. Palmer. 1994. Effects of manipulated diet on size and performance of brachyuran crab claws. Science 264:710–712.

Snell-Rood, E. C., J. D. Van Dyken, T. Cruickshank, M. J. Wade, and A. P. Moczek. 2010. Toward a population genetic framework of developmental evolution: the cost, limits, and consequences of phenotypic plasticity. Bioessays 32:71–81.

Thompson, D. W. 1917. On growth and form. Cambridge Univ. Press, Cambridge, U.K.

Van Wassenbergh, S., J. A. Strother, B. E. Flammang, L. A. Ferry-Graham, and P. Aerts. 2008. Extremely fast prey capture in pipefish is powered by elastic recoil. J. R. Soc. Interface 5:285–296.

Vincent, O., C. Weißkopf, S. Poppinga, T. Masselter, T. Speck, M. Joyeux, C. Quilliet, and P. Marmottant. 2011. Ultra-fast underwater suction traps. Proc. R. Soc. Lond. Ser. B-Biol. Sci. 278:2909–2914.

Wagner, G., and L. Altenberg. 1996. Perspective: complex adaptations and the evolution of evolvability. Evolution 50:967–976.

Wagner, G. P. 1996. Homologues, natural kinds and the evolution of modularity. Am. Zool. 36:36–43.

Waxman, D., and J. R. Peck. 1998. Pleiotropy and the preservation of perfection. Science 279:1210–1213.

Williams, T. A., and L. M. Nagy. 2001. Developmental modularity and the evolutionary diversification of arthropod limbs. J. Exp. Zool. Part B: Mol. Develop. Evol. 291:241–257.

Wills, M. A. 2007. Fossil ghost ranges are most common in some of the oldest and some of the youngest strata. Proc. R. Soc. Lond. Ser. B-Biol. Sci. 74:2421–2427.

Yang, Z. H., and B. Rannala. 2006. Bayesian estimation of species divergence times under a molecular clock using multiple fossil calibrations with soft bounds. Mol. Biol. Evol. 23:212–226.

Zack, T. I., T. Claverie, and S. N. Patek. 2009. Elastic energy storage in the mantis shrimp's fast predatory strike. J. Exp. Biol. 212:4002–4009.

Zelditch, M. L., D. L. Swiderski, H. D. Sheets, and W. L. Fink. 2004. Geometric morphometrics for biologists: a primer. Elsevier Academic Press, New York.

Zelditch, M. L., A. R. Wood, and D. L. Swiderski. 2009. Building developmental integration into functional systems: function-induced integration of mandibular shape. Evol. Biol. 36:71–87.

Associate Editor: R. Dudley

Appendix

Table A1. The number of species and specimens sampled for each superfamily.

Superfamily	Species (number of specimens measured)
Hemisquilloidea	*Hemisquilla australiensis (6), Hemisquilla californiensis (8)*
Pseudosquilloidea	*Pseudosquilla ciliata (6), Pseudosquillisma oculata (7), Pseudosquillana richeri (6), Raoulserenea hieroglyphica (5)*
Lysiosquilloidea	*Acaenosquilla acerba (2), Acanthosquilla derijardi (3), Alachosquilla digueti (6), Alachosquilla floridensis (6), Acanthosquilla multifasciata (6), Austrosquilla osculans (6), Acanthosquilla tigrina (1), Austrosquilla tsangi (5), Austrosquilla vercoi (2), Alachosquilla vicina (1), Bigelowina biminiensis (7), Bigelowina phalangium (6), Bigelowina septemspinosa (3), Hadrosquilla edgari (2), Hadrosquilla perpasta (6), Heterosquilla tricarinata (2), Kasim insuetus (1), Lysiosquillina lisa (2), Lysiosquillina maculata (6), Lysiosquilloides siamensis (2), Lysiosquillina sulcata (4), Lysiosquilla tredecimdentata (6)*
Parasquilloidea	*Faughnia formosae (6), Faughnia serenei (5), Pseudosquillopsis marmorata (6)*
Squilloidea	*Areosquilla alis (1), Areosquilla carinicauda (1), Anchisquilla chani (3), Alima neptuni (10), Busquilla plantei (5), Fallosquilla fallax (1), Harpiosquilla harpax (6), Harpiosquilla raphidea (6), Kempina mikado (6), Quollastria gonypetes (6), Quollastria subtilis (6), Squilla empusa (6)*
Gonodactyloidea	*Chorisquilla brooksii (6), Chorisquilla excavata (4), Chorisquilla gyrosa (6), Chorisquilla spinosissima (5), Echinosquilla guerinii (8), Gonodactylus chiragra (6), Gonodactylaceus falcatus (6), Gonodactylus platysoma (6), Gonodactylus smithii (6), Haptosquilla stoliura (6), Mesacturoides fimbriatus (4), Neogonodactylus bredini (6), Odontodactylus havanensis (6), Odontodactylus scyllarus (6), Taku spinosocarinatus (3)*